Polymer Degradation and Stability 119 (2015) 35–45

Contents lists available at ScienceDirect

Polymer Degradation and Stability

journal homepage: www.elsevier.com/locate/polydegstab

Poly(butylene succinate) and poly(butylene succinate-co-adipate) for food packaging applications: Gas barrier properties after stressed treatments

Valentina Siracusa [a, *], Nadia Lotti [b], Andrea Munari [b], Marco Dalla Rosa [c]

[a] Department of Industrial Engineering (DII), University of Catania, Viale A. Doria 6, 95125 Catania, CT, Italy
[b] Dipartimento di Ingegneria Civile, Chimica, Ambientale e dei Materiali, Università di Bologna, Via Terracini 28, 40131 Bologna, Italy
[c] Interdepartmental Centre for Agri-Food Industrial Research, Alma Mater Studiorum, University of Bologna, Department of Food Science, Piazza Goidanich 60, 47023 Cesena, FC, Italy

ARTICLE INFO

Article history:
Received 19 February 2015
Received in revised form
10 April 2015
Accepted 27 April 2015
Available online 7 May 2015

Keywords:
Biodegradable polymer
Gas transmission behavior
Thermo-degradation
Photo-degradation
Food packaging

ABSTRACT

Aliphatic polyester resins present the versatility of common plastics and are characterized by a good stability under ordinary conditions. They have acquired significant interest as environmentally friendly thermoplastics for a wide range of application, like food packaging field. We have investigated the permeability behavior of commercial poly(butylene succinate) (PBS) and poly(butylene succinate-co-adipate) (PBSA) polymers after food contact simulants and photo and thermal-oxidative degradation processes. Each stressed treatment was applied on thin film. Barrier properties to different gases (oxygen and carbon dioxide) were evaluated, showing that the chemical composition of the polymer strongly influenced the permeability to the gasses. Further, the same samples were tested at different temperatures, from 5 °C to 40 °C, in order to understand the effect of the temperature on the permeability behavior, and to calculate the process activation energy. Relations that bind the diffusion coefficients (D) and solubility (S) with temperature were studied. Differential Scanning Calorimetry (DSC) and FT-IR analyses were carried out in order to establish a correlation between permeability and sample structure/crystallinity. Negligible changes were evidenced in the polymers by means of DSC and FTIR measurements indicating structural stability of the polymers under process conditions. Gas barrier behavior, instead, resulted mainly affected by the process conditions, because mainly dependent on several chemical–physical factors. In both cases, no severe damage of the materials was observed.

1. Introduction

Packaging represents over 60% of the total plastic waste produced in Europe: many different polymers are currently employed in this field, both in contact or not with the food, such as polyolefins and poly(ethylene terephthalate), to cite only few examples. These traditional polymers are widely used in the packaging industry because of their good performances and relatively low cost; however, they possess very slow degradability in marine and terrestrial environments. Moreover, due to the contamination with organic matter, recycling of these materials is impracticable and economically not convenient [16,39]. As a consequence, thousands of tons of plastic packaging wastes are disposed in landfills every year, causing a continuous pollution increment, besides various municipal waste management problems. Therefore, the need of an alternative to these traditional materials is becoming more and more urgent. In this view, in recent years both academic and industrial researchers focused their attention on the use of biodegradable materials. To date, synthetic aliphatic polyesters represent one of the most economically competitive biodegradable polymers, being readily susceptible to biological attack [29]. In addition, they have attracted considerable attention as they combine the just mentioned features with interesting physical and chemical properties.

The performance expected from bioplastic materials used in food packaging application is protecting it from the environment, maintaining of course food quality [2]. These requirements can be achieved through a control and modulation of polymer

* Corresponding author. Current address: University of Catania, Engineering Faculty, Department of Industrial Engineering (DII), Viale A. Doria 6, 95125 Catania, Italy. Tel.: +39 0957382755; fax: +39 095337994.
E-mail address: vsiracus@dmfci.unict.it (V. Siracusa).

http://dx.doi.org/10.1016/j.polymdegradstab.2015.04.026
0141-3910/

chemical–physical, mechanical and barrier properties, which in turn depend on the structure of the polymeric packaging material. In addition, it is important to study the changes of the bioplastics that can occur during the interaction with the food [37].

At present, only Polylactic acid (PLA) is commercially used for food contact packaging application. Its properties can be well modulated in function of its use. The only negative point is the price, still much higher than that of the traditional plastics. Because of this limitation, PLA is actually employed principally in market niche, with high-value's food, like for example biological products, where the high price of the material packaging is justified by the high food price.

Poly(butylene succinate) (PBS) and Poly(butylene succinate-co-adipate) (PBSA) are two of the main candidate as aliphatic biodegradable polyesters to be used in the food packaging field. To improve their mechanical properties high molecular weight polymer/copolymer systems were prepared [8,14,15,25,29] by using particular catalysts or by; introducing a rigid aromatic structure into aliphatic copolyesters, or by preparing nanocomposites blend [4,28]. Their biodegradability, as well as, the influence of chemical structure on biodegradability has been widely investigated [31,43].

In view of a possible application of these two commercial aliphatic polyesters in the food packaging, it is fundamental to evaluate the compatibility of these materials with the food, in terms of loss in food quality properties. To do that, the permeability behavior is crucial in terms of shelf-life food study, to prolong the maintenance of organoleptic and nutritive characteristics and to preserve food from contamination.

In the present paper we describe the permeability behavior, and evaluate its changes after contact with foods or after photo and thermo oxidative processes. To mimic the food contact, we used four simulant liquids provided by law [standards Regulation (EC) No 1935/2004[32] and Regulation (EU) No 10/2011[33]]. Then, we performed a stressing degradation process by simulating an accelerating aging, by a thermo- and photo-exposition. The temperatures selected for accelerated experiments were those suggested by Robertson (2006) [34]; as the most suitable for accelerated test on food [35]. The percentage of ambient relative humidity was an averaged value among those recorded inside a supermarket within a solar year [34], and the value with the less influence on fat food oxidation rate [24].

2. Materials and methods

2.1. Materials

Poly(butylene succinate) (PBS) and Poly(butylene succinate-co-adipate) (PBSA), with the trade name of Bionolle, were kindly supplied and used as received from Showa Denko. The granules were transformed in thin films by thermal forming.

The gases used in the experiment are the ones normally employed for Modified Atmosphere Packaging solution (MAP, food grade purity).

2.2. Film preparation and thermal degradation procedure

Films of PBS and PBSA were obtained by hot pressing the polymers granules between Teflon sheets in a Carver press for 2 min at a temperature T equal to $T_m + 40$ °C. The films were cooled to room temperature in press by using running water. Before analysis, the films were stored at room temperature for at least two weeks in order to attain equilibrium crystallinity.

The film thickness was determined using the Sample Thickness Tester DM-G, consisting of a digital indicator (Digital Dial Indicator), connected to a computer. Reading was made twice per second (the tester performs automatically three readings, minimum value that cannot be changed), measuring a minimum, maximum, and average value of a series of measures. The reported results are an average of three experimental tests run at 10 different points on the polymer film surface, at room temperature. Measurements were performed at least in triplicate and the mean value thickness is presented.

The samples were exposed to thermal degradation and photo-degradation, simulating the supermarket light exposition. The thermal degradation was performed by a Constant Climate Chambers with Peltier Technology, model HPP 108/749, Memmert GmbH + Co. KG, P.O. Box 1720 D-91107 Schwabach Germany, at 40 °C and 50% of relative humidity (RH). The photo-degradation was performed by exposing the polymer film sample to a Philips fluorescent Tube TL-D 18W/33-640 1SL cool white (4100 K colour temperature, 63 Ra8 CRI Index, 1200 Lumen) at 23 °C (ambient temperature) and 50% of RH. This light exposer was home made thermostat instrument, with a temperature and light manual controller. Times of exposition ranged from 0 to 55 days. Film samples were exposed at a distance of about 30 cm.

2.3. Molecular characterization

2.3.1. Nuclear magnetic resonance (NMR)

The polymer structure and copolymer composition were determined by means of ^{1}H NMR spectroscopy. The samples were dissolved in chloroform-d solvent with 0.03% (v/v) tetramethylsilane added as an internal standard. ^{1}H NMR spectra were recorded at room temperature for solutions with a polymer concentration of 0.5 wt% (a relaxation delay of 1 s, an acquisition time of 1 s and up to 64 repetitions). A Varian INOVA 400 MHz instrument was employed for the measurements.

2.3.2. Gel permeation chromatography (GPC)

Molecular weight data were obtained by GPC at 30 °C using a 1100 Hewlett Packard system equipped with a PL gel 5m MiniMIX-C column (250 mm/4.6 mm length/i.d.) and a refractive index detector. In all cases, chloroform was used as eluent with a 0.3 ml min^{-1} flow and sample concentrations of about 2 mg ml^{-1} were applied. Polystyrene standards in the range of molecular weight 2000–100 000 were used.

2.4. Simulant liquid

Aqueous food, acid food, aqueous food containing oil/fat, acid food containing oil/fat, oily or fatty food, alcoholic food and low-moisture content solid food are the possible contact scenario [5]. The food contact simulation was performed in accordance with [32] Regulation (EC) No 1935/2004 of the European parliament and of the council of 27 October 2004 on materials and articles intended to come into contact with food and in accordance with the Union Guidelines [33] Regulation (EU) No 10/2011 on plastic materials and articles intended to come into contact with food. Four substances were used as food simulants:

- Simulant A, distilled water, at 40 °C for 10 days;
- Simulant B, Acetic Acid 3%v/v, at 40 °C for 10 days;
- Simulant C, Ethanol 10% v/v, at 40 °C for 10 days;
- Simulant D, Isooctane at 20 °C for 2 days.

The test simulant contact time investigated the extreme contact conditions between packaging and product. The measurement was made by total immersion of about 8 cm × 8 cm film specimen. 100 ml of simulant was placed into glass flasks (of 150 ml of volume) containing the specimens and the flasks were then covered

with caps. After the assay time was completed, the specimens were removed from the flasks, washed with distilled water two times and dried with blotting paper. Before analysis, the films were kept at room temperature, in dry ambient for at least two weeks, in order to attain equilibrium crystallinity. Each material was tested in triplicate.

2.5. Permeability measurement

The permeability determination was performed by a manometric method using a Permeance Testing Device, type GDP-C (Brugger Feinmechanik GmbH), according to ASTM 1434-82 (Standard test Method for Determining Gas Permeability Characteristics of Plastic Film and Sheeting), DIN 53 536 in accordance with ISO 15105-1 and according to [11] Gas Permeability Testing Manual (Registergericht München HRB 77020, Brugger Feinmechanik GmbH). The equipment consists of two chambers between which the film is placed. The upper chamber is filled with the dry test gases at ambient pressure. The permeation at the bottom chamber of the test specimen is determined by the evaluation of the increase in pressure in the previously evacuated volume. The increase in pressure during the test period is evaluated and displayed by a PC. Fluctuation of the ambient temperature during the test was controlled by special software, with an automatic temperature compensation, which minimizes Gas Transmission Rate (GTR) deviations. The recorded temperature fluctuations and the calculated GTR values are correlated using a temperature depending correction factor, which is found by the software automatically.

The film sample of 2 × 2 cm in size was placed between the top and the bottom of the permeation cell, using a film mask to cover the remaining surface area. The GTR value, that is the Rate of the film Gas Transmission, was determined considering the increase in pressure in relation to the time and the volume of the device. The pressure is given from the instrument in (Bar) units. To obtain the data in kPa, the primary SI units, it is necessary to use the following correction factor: 1 Bar = 100 kPa, according to NIST special publication 811 (NIST 2008) [30,40].

Time Lag (t_L), Diffusion coefficient (D) and Solubility (S) of the test gases into the film under study were measured in addition to GTR value. The mathematical relations used are well reported on literature [27,40,41].

The operative conditions were: room condition temperature of 23 °C; gas stream of 100 cm^3/min; 0% of Gas RH; sample area of 0.785 cm^2.

Method A was used for the analysis, as just reported in the literature [9,27,11,40], with evacuation of top/bottom chambers.

For the determination of the activation energies of the permeation process, films were analyzed at a temperature of 10, 20, 30 and 40 °C, using dry gases (O_2 and CO_2) at 0% RH. Sample temperature was set by an external thermostat (KAAKE-Circulator DC10-K15 type, Thermoscientific, Selangor Darul Ehsan, Malaysia).

All experiments were performed in triplicate and a good reproducibility was achieved. The mean value is presented.

2.6. Differential scanning calorimetry (DSC) measurements

The temperatures of the thermal characteristic transitions of polymers and the changes in crystal/amorphous ratio were estimated calorimetrically by means of a Perkin–Elmer type Pyris DSC-6 differential scanning calorimeter, equipped with a liquid sub ambient accessory and calibrated with high purity standards such as Indium and Tin. Polymer films were cut into small pieces of 2 mm^2 and placed in a 50 μL sealed aluminium crucibles. Samples of about 10–12 mg have been prepared. In order to avoid film contamination, special care was taken during handling, working with gloves and tweezers. All tests were run under pure nitrogen flow (20 cm^3 min^{-1}). After an isotherm of 5 min at −30 °C, weighed samples were heated, with a scanning rate of 10 °C min^{-1}, from −30 to 125 °C and 135 °C, for PBSA and PBS, respectively. Subsequently, after rapid quenching, the samples were reheated at the same condition of the first scanning rate. All experiments were performed under a nitrogen flow (20 cm^3 min^{-1}), in triplicate.

The glass-transition temperature T_g was taken as the midpoint of the heat capacity increment Δc_p associated with the glass-to-rubber transition. The melting temperature (T_m) and the crystallization temperature (T_c) were determined as the peak value of the endothermal and the exothermal phenomena in the DSC curve, respectively. When multiple endotherms were observed, the highest peak temperature was taken as T_m. The specific heat increment Δc_p, associated with the glass transition of the amorphous phase, was calculated from the vertical distance between the two extrapolated baselines at the glass transition temperature. The heat of fusion (ΔH_m) and the heat of crystallization (ΔH_c) of the crystal phase were calculated from the total areas of the DSC endotherm and exotherm, respectively. For each sample the crystallinity degree was evaluated according to the following formula: x_c (%) = ($\Delta H_m/\Delta H_m^*$) 100, where ΔH_m is the melting enthalpy calculated from the experimental curve while ΔH_m^* is the melting enthalpy of 100% crystalline sample, equal to 110.3 J g^{-1} for PBS and 135.0 J g^{-1} for PBSA films, as reported from literature [29,44–46] T_c and T_m values are well reproducible from the second scan, while those relating to the first scan are affected by thermal and mechanical history to which the samples were subjected.

2.7. FTIR spectroscopic analysis

The FT-IR/ATR spectra were recorded on sample films by a Perkin-Elmer-1725-X Spectrophotometer (Labexchange Group, Burlandingen, Deutschland). Spectra were recorded from 4000 cm^{-1} to 600 cm^{-1} with a resolution of 4.0 cm^{-1}. The results are an average of 10 experimental tests, run on 10 different samples point to test the results' reproducibility. 64 scan were recorded on each sample. The experiments were performed at room temperature, directly on the samples, without any preliminary treatments.

2.8. Statistical analysis

One-way analysis of variance (ANOVA) and test of mean comparisons according to Fisher's least significant differences (LSDs) were applied on obtained results, with a level of significance of 0.05. The statistical package STS Statistical for Windows, version 6.0 (Statsoft Inc., Tulsa, Okla., U.S.A.) was used. Values are given as mean ± SD of 3 replicates.

3. Results and discussion

The chemical structure of the two homopolymers is reported in Fig. 1

The two homopolymers are characterized by the same glycol sub-unit, but different acid sub-unit, the adipic one being surely more flexible having a higher number of methylene groups.

3.1. Molecular and thermal characterization data

Before studying permeability behavior, the two commercial polymers have been subjected to an accurate molecular and thermal characterization.

As an example, the ^1H NMR spectrum of PBSA copolymer is reported in Fig. 2: as it can be seen, it is consistent with the expected structure. The copolymer composition, calculated from the

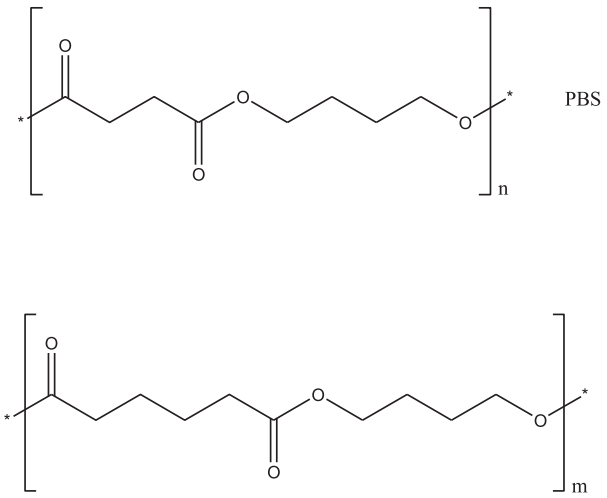

Fig. 1. Chemical structures of Polybutilene succinate (PBS) and Polybutylene adipate (PBA) homopolymers.

relative areas of the ^{1}H NMR resonance peak of the **a'** aliphatic proton of the adipic subunit located at 2.33 ppm and of the **a** protons of the succinic subunit at 2.61 ppm turned out to be 80 mol % of Butylene Succinate (BS) co-units.

The molecular weights are collected in Table 1: the copolymer is characterized by a significant lower molecular weight compared to the homopolymer PBS; in both cases, the polydispersity is typical of polyesters.

DSC was used to investigate the thermal transitions occurring in the polymers, (see data in Table 1). Both PBS and PBSA film are semicrystalline, with T_g values below RT and function of composition: the insertion of BA co-units into PBS macromolecular chains causes a lowering of glass transition temperature due to the higher chain flexibility of BA co-units with respect to BS ones. Above T_g, the DSC heating scan of PBS shows a premelting followed by a cold crystallization peak (data not shown), which can be attributed to crystal phase rearrangements, and finally a melting peak (T_m = 112 °C). The DSC curve of PBSA displays a broad melting endotherm with a peak (T_m) at 95 °C corresponding to the fusion of the crystal phase developed by BS units. The significantly lower value of both T_m and melting enthalpy (ΔH_m) in the case of the copolymer indicates the reduced level of crystallinity in PBSA compared to PBS.

3.2. Barrier properties

Carbon dioxide and oxygen are two of the main permeates studied in packaging application, especially in Modified Atmosphere Packaging application (MAP technology), because they may transfer from the internal or external environment through the polymer packaging wall, influencing continuously the product quality and shelf-life. Therefore, gas permeation studies are essential to understand and estimate its utility for food preservation [42]. As it is well known from literature, several factors can influence the barrier properties of packaging materials [36,42]. By reviewing scientific literature of the investigated field, the gas permeation through polymers is described by a diffusion model, using Henry and Fick's laws, obtaining the expression that relates the permeation rate with the area and thickness of the film [22,34]. The correlation between the term *Permeability* (or permeability coefficient or permeation coefficient), which is referred to the product between Diffusivity (D) and Solubility (S) coefficients (DS), and which is represented by the symbol P, and *permeance* and *thickness* (X) is well known [34]. The P/Xratio (with X = total thickness of the polymer film) is called *permeance*, and represents the total amount of protection afforded by unit area of a barrier material. This value approaches to zero only asymptotically. Consequently the permeability coefficients (P, D and S) are independent to the thickness (because the thickness is already accounted for in the calculation of P) only if polymer thickness X increases beyond a certain value. It is at this point that it becomes

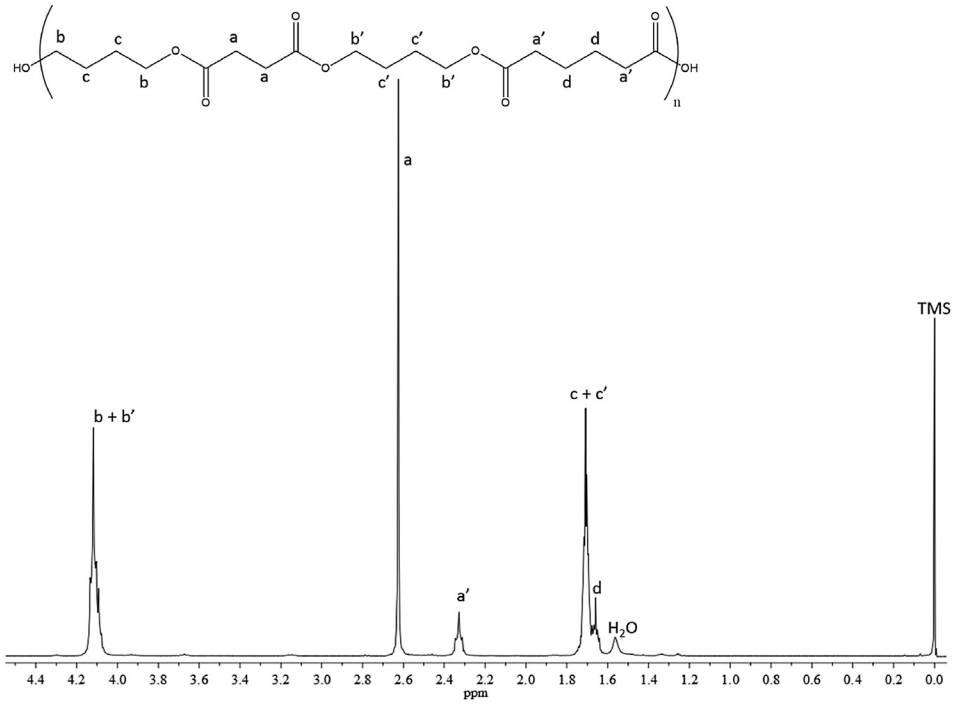

Fig. 2. ^{1}H NMR spectrum of PBSA copolymer.

Table 1
Molecular and thermal characterization data of PBS and PBSA.

				I scan			
Polymers	M_n	PDI	BS (mol %)	T_g (°C)	Δc_p (J/°C g)	T_m (°C)	ΔH_m (J/g)
PBS	66590	2.17	100	−35	0.0268	112	57
PBSA	29100	2.07	80	−45	0.0667	95	31

uneconomical to further increase film thickness with the aim of obtaining lower permeability levels. The standard equation used to calculate the permeability of a polymer material is based on: 1) the calculation of D and S under steady-state conditions (a gas will diffuse through a polymer at a constant rate if constant pressure difference is maintained across the polymer); 2) the linearity of gas concentration-distance relationship through the polymer; 3) the assumption that diffusion takes place in one direction only; and 4) the independency of D and S from the gas concentration. Like all simplifying assumptions, there are many instances where they are not valid. In practice deviations occur. The permeability behavior is than described by the Transmission Rate (TR) of the material: $TR = Q/At$ where Q is the amount of permeant passing through the film (cm^3), A is the sample area (cm^2) and t is the time (day). Permeability of polymers to organic compound or water is often presented in this way and the term GTR (Gas Transmission Rate) is of common usage [22,34].

In our work, we correlate the permeability data, expressed as GTR, S, D and t_L with the permeability main influencing factors in the case of unstressed (standard) and stressed samples (simulant liquids; thermo and photo-degraded), the temperature effect being considered as well. GTR values, together with S, D and t_L of the tested gases are reported in Table 2, for O_2 and CO_2 pure gas, respectively. Thickness and selectivity ratio were also reported. Our results confirm that the CO_2 permeability value is greater than that of O_2, the difference entity changing according to the polymer. This dependence was expressed by the corresponding *selectivity ratio*, which is very high for the PBS sample, indicating a high correlation with the chemical structure factor. For the PBS sample there is a very big difference on the CO_2–O_2 GTR data: CO_2 GTR is 10 times higher than O_2 one. For the PBSA sample this difference is lower, with a CO_2 GTR value about 3.6 times higher than the O_2 one. This different behavior can be correlated to the different chemical structure of the two materials. As can be observed from the chemical formulas reported in Fig. 1, and from the T_g values reported in Table 1 PBSA chain is more flexible than PBS, giving rise to a more tortuous path for the gas molecules, which spent more time inside the material. This is confirmed by the D, S and t_L data. S value, which expresses the volume solubility of the gas dissolved in one volume of polymer material, and D value, correlated to the gas molecules speed through the polymer, are the permeability parameters influenced by the chemical structure of the polymer. For PBS sample the S value with CO_2 gas is about 245 times higher, indicating more compatibility of this gas with the polymer than for O_2 gas. Consequently the D value is lower with CO_2 because the gas molecules spent more time to cross the film. The time to reach the steady-state is longer for CO_2 because molecules takes more time to homogeneously arrange inside the polymer backbone, due to their faster and very chaotic motion. The D, S and t_L data were not recorded for the PBSA sample because was not possible to fit the slope of the linear portion of the obtained curve [1]. Permeability results here presented are of particular relevance if we compare the permeability of the PBS and PBSA samples with those of PLA films obtained under the same conditions. As reported in Table 2, PBSA shows lower GTR, and therefore improved barrier properties, to both CO_2 and O_2 gases with respect to polylactide, while PBS is characterized by a lower permeability just to O_2 gas but higher to CO_2 gas test. It is worth remembering that PLA is the most extensively used polyester in the production of biodegradable packaging films and that is possible to choose the best packaging solution selecting the appropriate permeability.

GTR data after food simulant contact for PBS and PBSA film are reported in Table 3. As can be observed they change in a different way: PBS sample shows an increment of the GTR value, with the highest value recorded when ethanol is used. PBSA on the contrary shows a decrement of the GTR value, especially after acetic acid contact. Although there are not big differences in the chemical structure of the two polymers, the interaction with the ambient is different. Materials that are good barriers when dry, can behave badly when tested in a different ambient than in service, like water. On the other side, for low barrier film, the medium reduces the gas transmission. For the highest barrier materials, like for example poly(vinylidene-chloride) (PVDC) the medium's influence on gas transmission is almost undetectable [10]. According to the literature [6], under the action of water the polymer swells and changes its structure making diffusion of gases easier. This behavior was observed for PBS sample that showed high GTR values regardless the type of food simulants being used. Permeability of PBSA, less hydrophilic that PBS, changed giving rise to a less diffusion of gases through the polymer wall, due probably to a plasticizing effect which makes un obstacle to the gas motion.

D and t_L data, determined only for PBS sample, followed perfectly the GTR value recorded: when GTR increases, D increases and t_L decreases. It means that if the gas transmission increases, the molecules diffuse more rapidly through the film and consequently less time is necessary to reach the steady-state of the transmission process. S value instead shows a not regular trend. In theory if the GTR value increases, S should decrease, according to a lower

Table 2
GTR, S, D and t_L for O_2 and CO_2 gas, thickness and selectivity ratio of the films.

Sample/Permeability parameters	PBS	PBSA	PLA*
O_2			
GTR (cm^3/m^2 d bar)	281.00 ± 0.00	131.93 ± 4.20	487.67 ± 2.52
S (cm^3/cm^2 bar)	$4.48E^{-03} \pm 2.76E^{-03}$	n.a.	
D (cm^2/s)	$6.74E^{-07} \pm 9.87E^{-08}$	n.a.	
t_L (s)	52.67 ± 7.85	n.a.	
CO_2			
GTR (cm^3/m^2 d bar)	2866.66 ± 20.55	469.47 ± 1.58	1201.00 ± 1.73
S (cm^3/cm^2 bar)	$1.1E^{+00} \pm 0.06$	n.a.	
D (cm^2/s)	$4.34E^{-08} \pm 1.22E^{-09}$	n.a.	
t_L (s)	808.00 ± 22.23	n.a.	
Thickness (μm)	144.67 ± 2.10	339.03 ± 3.61	
Selectivity ratio (CO_2/O_2)	10.20	3.56	

n.a. = not analyzed; * PLA1 from Literature [41].

Table 3
GTR, S, D and t_L data after Food Simulant contact for PBS film and GTR increment for PBSA film.

Food simulants/Permeability parameters	Standard	Distilled water	Acid acetic	Ethanol	Isooctane
GTR (cm^3/m^2 d bar)	2867 ± 20.55	3550 ± 0.00	4330 ± 0.00	5417 ± 4.71	3910 ± 8.16
S (cm^3/cm^2 bar)	$1.10E^{+00}$ ± 0.06	$1.15E^{+00}$ ± 0.02	$3.23E^{-01}$ ± 0.46	$7.52E^{-01}$ ± 0.00	$1.36E^{+00}$ ± 0.01
D (cm^2/s)	$4.34E^{-08}$ ± $1.22E^{-09}$	$5.19E^{-08}$ ± $7.59E^{-09}$	$7.49E^{-8}$ ± $9.43E^{-11}$	$1.21E^{-07}$ ± 0.00	$4.82E^{-08}$ ± $1.63E^{-10}$
t_L (s)	808 ± 22.23	675 ± 9.74	467 ± 0.47	289 ± 0.00	727 ± 2.49
GTR increment PBS (%)	0	24	51	89	36
GTR increment PBSA (%)	0	−32	−41	−26	−38

compatibility between polymer and gas molecule. We observed this trend for acetic acid and ethanol simulants but not for distilled water and isooctane simulants where S value increased (see Table 3). On Table 3 was reported also the % increment or decrement of the GTR value for PBS and PBSA films, in respect to the simulant liquids. As can be noted the highest increment was recorded for the PBS sample, showing a higher interaction with the ambient (polar or not). This behavior was subsequently explained by thermal analysis results: a decrement of cristallinity percentage was recorded, with subsequent increment of GTR value. On the contrary, for PBSA sample decrements on GTR values were observed in respect to the standard film. The decrease is due to a swelling effect that creates an obstacle to the gas molecules to cross the film wall, when in contact with the simulant liquids.

After thermo and photo-degradation a change was observed on the gas transmission behavior, more intense after photo-degradation than after thermo-degradation. Both treatments were made stressing the environmental ambient, the first one simulating the supermarket exposition and the second one an acceleration degradation process, which correspond to an ageing of 0.7–8.3 solar years (365 days after the first exposition, so 255.5–3029.5 days of ageing), as calculated also from Koutny [20] for the biodegradation study of polyethylene films with pro-oxidant additives [20,17]. Data recorded are reported on Fig. 3, with the corresponding linear regression coefficient (R^2) of the corrected experimental point fittings. For PBS sample, as can be observed from the figure, there is no good correlation between permeability and exposition time after thermal treatment (R^2 is equal to 0.20) but a little bit more linear result was obtained after photo-degradation process (R^2 is equal to 0.41). After 5 and 10 days, data do not fit with the theoretical line while after 15–55 days a more regular behavior was recorded. For PBSA sample a more linear trend was recorded: more linear result was obtained after photo-degradation treatments than for thermo-degradation (R^2 is equal to 0.76 and 0.52 respectively). Due to their different polymer structure it is evident that the two polymers are influenced differently by the environment. Change in crystallinity was recorded, which explain the different permeability behavior.

For PBS sample D, S and t_L were recorded and data were reported on Fig. 4. The following trend is respected for both treatments: an increase of GTR value is followed by a decrease in S value and an increase in D value, meaning that the permeability process is well correlated to the physical material modification recorded during the treatment. Data for PBSA sample was not recorded because was not possible to detect the t_L.

In order to describe the GRT dependence to the temperature, the Arrhenius model was used to calculate the activation energies for gas transmission (E_{GTR}), sorption (H_S) and diffusion (E_D) processes. The mathematical relations used are well reported in literature [26]. Activation energy is obtained by calculating the value from the slope ($-E_a R^{-1}$) of the Arrhenius equation, where R is the gas constant (8.314 J mol^{-1} K^{-1}). Natural logarithmic (*ln*) of GTR, S and D compared with inverse temperature were reported in Figs. 5–7 for O_2 and CO_2 gases, together with the indication of the calculated linear regression of the corrected experimental points fittings, with standard deviation. On Table 4 are reported the corresponding calculated activation energies for the permeability (E_P), Solubility (H_S) and Diffusivity (E_D) process, in the range 5–40 °C, for O_2 and CO_2 gas respectively, with the corresponding R^2 factor (between bracket).

In Fig. 5 the *ln* of GTR data as a function of temperature is reported. As it can be seen, the data fit the theoretical relation very well, with high R^2 coefficients, indicating a good correlation between permeability and temperature, for both gases. Permeability increases with increasing temperature. The corresponding E_{GTR} is very high, more for CO_2 than for O_2 gas test. This behavior confirms the assumption that CO_2 molecules move faster than O_2 gas molecule and so permeability to CO_2 is higher that O_2 one. lnS values, reported on Fig. 6, follow also a linear relationship, indicating a good correlation with the GTR data. The trend is different depending on the gas used. With O_2 gas, PBS shows a standard behavior, increasing the solubility with increasing the

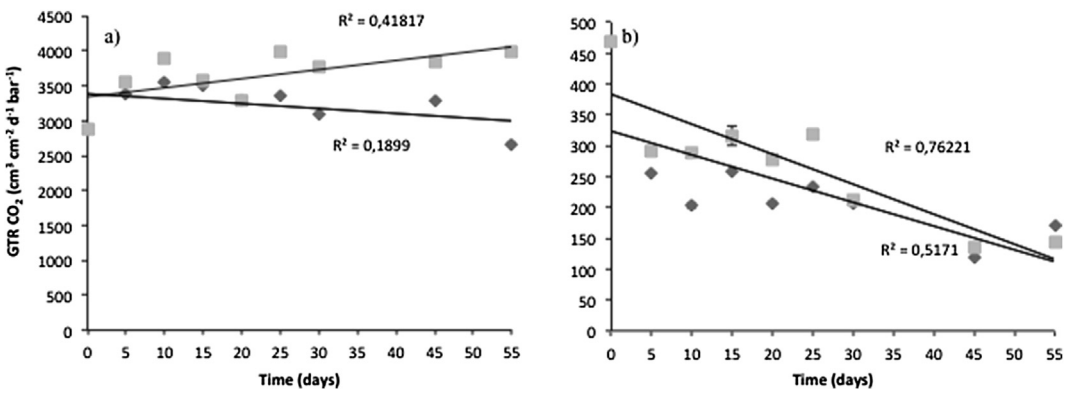

Fig. 3. GTR data for a) PBS and b) PBSA films, after (◆) thermo and (■) photo-degradation.

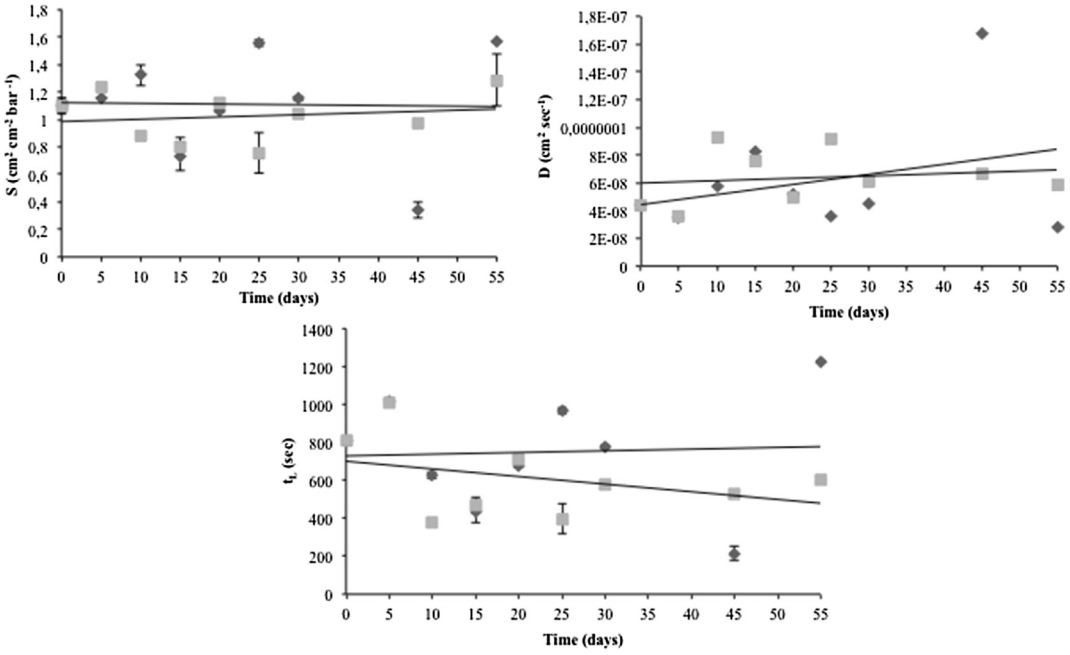

Fig. 4. S, D and t_L for PBS sample, after (◆) thermo and (■) photo-degradation.

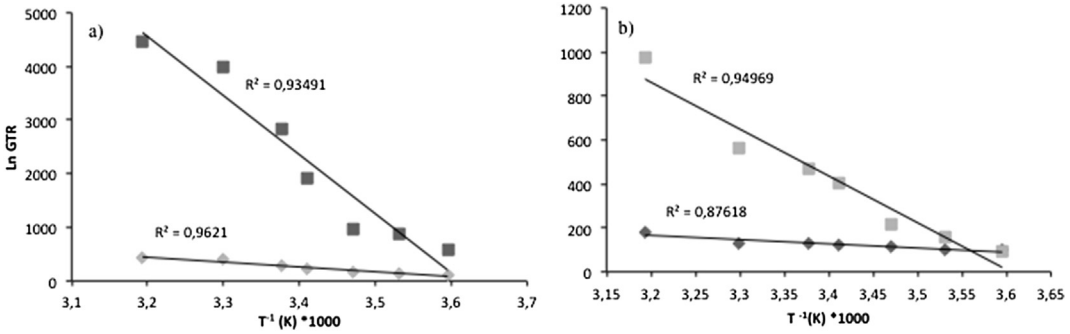

Fig. 5. Arrhenius plot of GTR coefficient for oxygen (◆) and carbon dioxide (■), for: a) PBS and b) PBSA samples.

temperature and consequently the permeability. With CO_2 gas the trend is opposite, as observed also from the Hs value recorded: the solubility decreases with increasing the temperature. The Solubility behavior is the parameter correlated to the polymer composition so this trend is a confirmation that the gases interact differently with the matrix. From low to high temperature the *ln*S value shifts with a scissors trend, and the corresponding H_S shows a fluctuant value, positive for O_2 gas test and negative for CO_2 gas test. *Ln*D (Fig. 7) shows a standard behavior for PBSA sample with O_2 gas test. For PBS sample *ln*D value

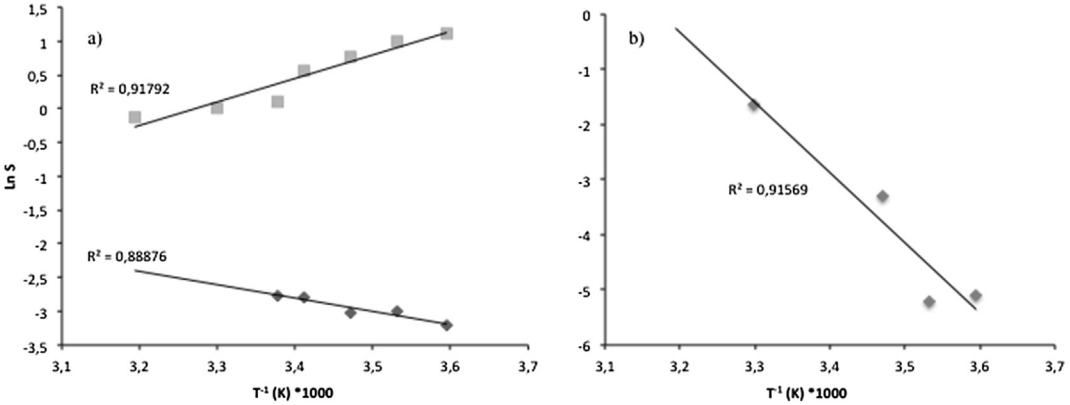

Fig. 6. Arrhenius plot of S coefficients for oxygen (◆) and carbon dioxide (■), for: a) PBS and b) PBSA samples.

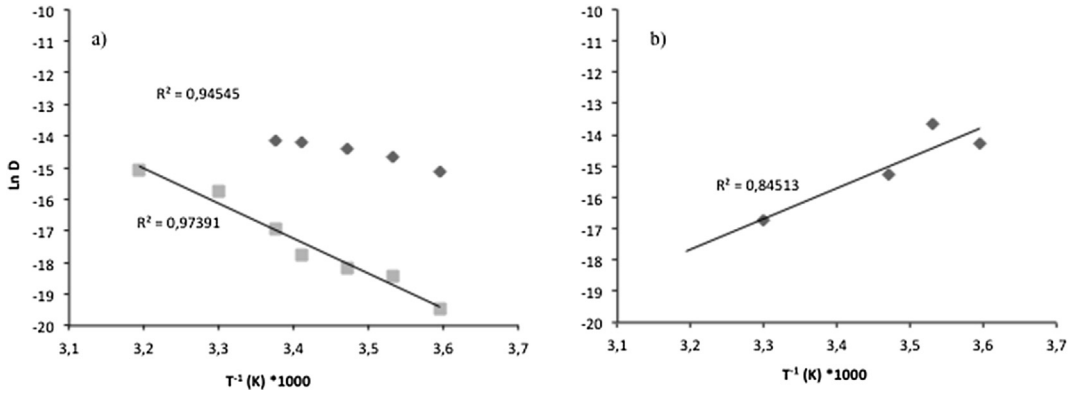

Fig. 7. Arrhenius plot of D coefficients for oxygen (◆) and carbon dioxide (■), for: a) PBS and b) PBSA samples.

Table 4
Activation Energies (E_{GTR}, H_S, E_D) data for O_2 and CO_2 gas in the 5–40 °C range and the linear regression coefficients (R^2) between bracket.

Sample (gas test)	E_{GTR} (kJ/mol)	H_S (KJ/mol)	E_D (kJ/mol)
PBS (CO_2)	91645.22 (0.935)	−28.94 (0.918)	92.15 (0.974)
PBS (O_2)	7475.12 (0.962)	16.44 (0.889)	35.90 (0.945)
PBSA (CO_2)	16628.00 (0.950)	105.69 (0.916)	−81.19 (0.845)
PBSA (O_2)	1603.58 (0.876)	–	–

shows the same trend for oxygen and carbon dioxide, thus meaning that the diffusion was the same for the tested gas, despite the different solubility. Consequently, E_D shows a positive value for both gas test. As is well known from literature [3], high activation energy implies more sensibility to temperature variation. We found that the permeation process is very well correlated to the temperature variation while the sorption/diffusion process shows consistent deviation, more correlated to polymer structure. Further, the corresponding selectivity ratio shows different value depending on the temperature, confirming that also this parameter is not a constant, and is correlated not only to the chemical structure of the materials, but depends also from the analysis temperature. Values were reported in Table 5.

3.3. Thermal analysis

Two consecutive scans were performed in order to know the melting temperature (T_m), the crystallinity degree (x_c) and the endotherm shape for the analysed materials. After heating, subsequent quenching and reheating, the thermal history of the samples was studied. On Table 6 are reported the thermal properties of the two standard polymer, as films and granules, and after contact with food simulants.

A slight increase of crystallinity was observed during the second scan, indicating the polymer ability to recrystallize. The degree of cystallinity was higher for PBS than for PBSA. During the first scan both polymers show a small melting peak before the main melting peak. For PBSA sample it was recorded at 74°C and 78 °C, for granule and film, respectively. For PBS sample it was recorded at 80°C and 100 °C. Such peak was ascribed to crystallite reorganization during heating [29].

After food simulant contact a difference on thermal behavior was recorded, for both polymers. As can be observed from data reported on Table 6, the X_c after simulants contact shows same changes. For PBS is more evident after ethanol contact. It can be observed that the X_c decreases from 46% to 20 %. As previously observed, this conspicuous decrement influenced the GTR behavior: in fact the permeability recorded was the highest, showing the well known dependence between crystallinity and permeation process [13]. When in contact with distilled water, acetic acid and isooctane, PBS shows a slight increment of crystallinity. The corresponding permeability value shows also an increment, not proportional and not correlated to the crystallinity increment. As reported from Jamshidian et al. 2012 [18]; theoretically high crystalline sample showed low permeability, with a very high dependence of the permeability data on the chemical–physical structure of the material. This trend is not always respected because in same cases the crystallinity has a reverse effect, leading to higher permeability because of the phenomenon of de-densification of the amorphous phase, which counteracts the decrease of the quantity of permeable amorphous phase due to crystallization [23]. A different behavior was observed for PBSA sample where a small decrement of the percentage of crystallinity was recorded, for all simulant contact samples. The GTR increases only when acetic acid was used, while in all other cases the value decreases despite of a reduction in crystallinity degree. This change in crystallinity percentage influenced especially the sorption/diffusion processes. The trend recorded was the same, for the 1st and the 2nd heating scan. For better understand the phenomena, the partially overlapped endotherms were deconvoluted into the component single peaks. As an example on Fig. 8 is reported the first and second DSC heating scan curve of the PBS film sample, after ethanol contact, with the corresponding first and second derivative function. The second derivative has been chosen as a criterion to assign the position of the melting peak maxima, as previously reported from Elvira et al. (2004) [7] in a DSC study of thermo-oxidized metallocene isotactic PP. This method gave us the possibility to detect all the endotherm components that in many cases are not conspicuous enough to be well detected, appearing on the thermogram as small/medium shoulders of the main peak. From the Figure it is evident that several peaks are present, due to

Table 5
Selectivity ratio for PBS and PBSA sample at different temperature.

Sample/Temperature	5 °C	10 °C	15 °C	20 °C	23 °C	30 °C	40 °C	R^2
PBS	5.19	6.65	5.46	8.39	10.08	10.11	10.25	0.778
PBSA	1.00	1.63	1.87	3.36	3.56	4.36	5.36	0.974

Table 6
Thermal data for PBS and PBSA.

	1st scan			2nd scan		
	ΔH_m (J/g)	Tm_1, Tm_2 (°C)	X_c (%)[a]	ΔH_m (J/g)	Tm_1, Tm_2 (°C)	X_c (%)[a]
PBS						
Film	51 ± 6	100 ± 0.02 113 ± 0.04	46	57 ± 7	102 ± 0.03 113 ± 0.04	51
Granule	54 ± 1	80 ± 0.01 115 ± 0.04	49	55 ± 0.6	113 ± 0.38	50
Distilled water	55 ± 0.2	101 ± 0.07 112 ± 0.04	50	55 ± 0.5	102 ± 0.00 113 ± 0.02	51
Acetic acid	54 ± 0.1	102 ± 0.01 113.51 ± 0.03	49	59 ± 0.06	101 ± 0.03 112.30 ± 0.06	53
Ethanol	22 ± 0.0	104 ± 0.02 115 ± 0.07	20	20 ± 0.06	102 ± 0.11 114 ± 0.01	18
Isooctane	55 ± 0.7	103 ± 0.03 114 ± 0.01	50	56 ± 0.01	102 ± 0.09 113 ± 0.04	50
PBSA						
Film	43 ± 0.3	78 ± 0.03 94 ± 0.04	32	45 ± 0.8	95 ± 0.06	34
Granule	45 ± 1.9	73 ± 0.06 95 ± 0.04	33	45 ± 0.1	94 ± 0.01	33
Distilled water	38 ± 0.2	– 94 ± 0.08	28	37 ± 0.02	94 ± 0.01	28
Acetic acid	41 ± 0.0	79 ± 0.05 95 ± 0.07	30	63 ± 0.06	94 ± 0.01	47
Ethanol	40 ± 0.07	77 ± 0.03 94 ± 0.05	30	43 ± 0.10	94 ± 0.02	32
Isooctane	42 ± 0.08	78 ± 0.03 93 ± 0.05	31	48 ± 0.05	93 ± 0.05	36

[a] Calculated by dividing the observed heat of fusion by the theoretical value calculated for 110.3 J/g and 135 J/g for PBS and PBSA respectively [29].

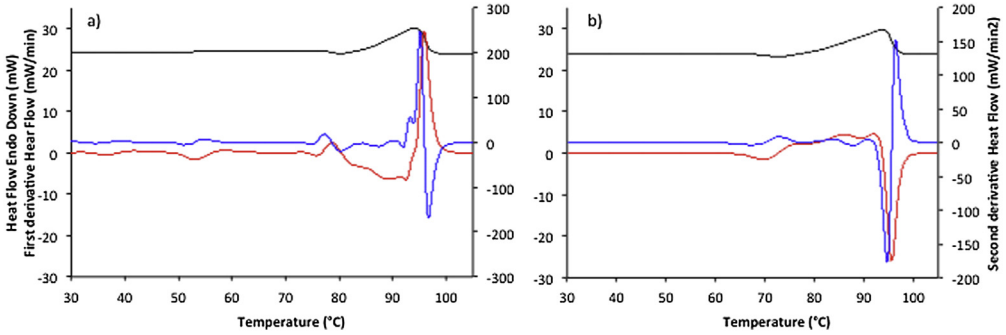

Fig. 8. 1st (red) and 2nd (blue) derivative of a) first and b) second DSC heating scans, of PBS film sample, after ethanol contact.(For interpretation of the references to colour in this figure legend, the reader is referred to the web version of this article.)

different polymer segments of different length that could influence the sorption/diffusion processes [9,21].

Thermal analysis of the no-aged film was used to confirm that processing did not significantly affect the properties or chain microstructure of the films. After thermo- and photo-degradation a negligible difference was observed in the T_m values, indicating that the molecular weight of the material do not change significantly during the degradation process. This suggested that crosslinking, which would have caused broadening and shifting of peaks to lower temperatures, was not significant during the aging. The highest T_m deviation was observed for the PBS sample with the highest X_c value, after 10 days of thermal degradation and 45 days of photo-degradation. On the contrary, the X_c values, reported in Fig. 9, show a different behavior depending on the stressed treatment and on the sample under analysis. For PBS sample, during thermo-aging a decrease of the highest temperature peak was observed, accompanied by a broadening of the endothermic peak. This can be associated to a chain scission process of the longest chains with formation of shorter sequences able of crystallizing. During the first heating scan the corresponding X_c value increased, ranging from 46 to 66%, depending on the exposition time. During the second heating scan the % of crystallinity increased further, indicating a high tendency of the sample to recrystallize after quenching. Similar behavior was observed from Gauthier et al. (2013) [12]; during their study of photo- and thermo-degradation of LLDPE-based films. During photo-aging there was a more linear increase in the relative X_c value, ranging from 46 to 63%, as indicated from the calculated linear regression coefficient (R^2) of the corrected experimental points fittings, reported on Fig. 10. The R^2 values were of 0.10 and 0.39, for thermo- and photo-degradation respectively, showing a better linear correlation between degradation time and physical modification in the case of photo-aging. Data recorded are well in accordance to the GTR results.

For PBSA sample a better linear behavior was observed, for both thermo- and photo-treatment, but during the aging time a small decrement of crystallinity was recorded, in the range 28–32%. The corresponding linear regression coefficient (R^2) of the corrected experimental points fittings was of 0.31 and 0.02 for thermo- and photo-degradation. Therefore, in the case of PBSA sample data fits well with degradation time in the 15–30 days range, while before

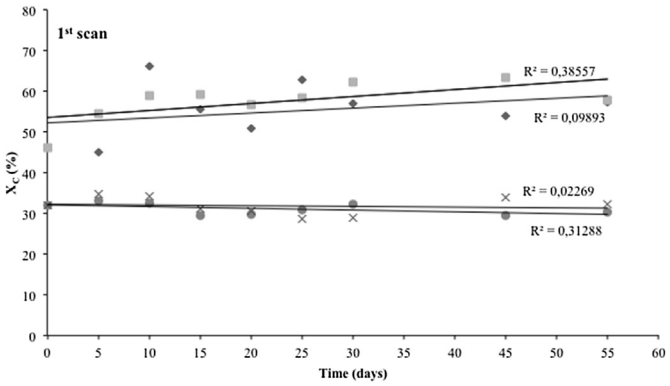

Fig. 9. Xc behavior for PBS film after thermo (◆) and photo (■) degradation and for PBSA film after Thermo (●) and Photo (×) degradation, during the first heating scan.

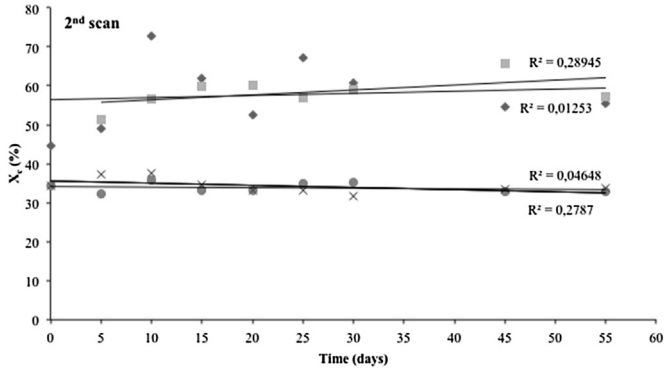

Fig. 10. Xc behavior for PBS film after thermo (◆) and photo (■) degradation and for PBSA film after Thermo (●) and Photo (×) degradation, during the second heating scan.

and after this time period a deviation is observed, indicating that crystalline reorganization is strictly dependent on the time. Interestingly, PBSA GTR values were higher than those of PBS despite X_c values for the copolymer were about a half of those of PBS. This peculiar result can be explained as due to a reduction in the interlamellar spacing, which promote the gas molecule film crossing. Similar results were observed from Kanehashi et collaborators (2010) [19] in their study of permeability behavior on 300 crystalline and liquid crystalline polymers, in a lower–higher crystalline range. These experiments suggest that at the beginning the degradation involve the longest polymer chains (lowering of the melting main peak) and then the shorter ones crystallize (broadening of the peak and crystallinity degree increase). The degradation process however depends on the polymer chemical structure and on the deteriorate treatment used. For PBS is more stressful the thermo-degradation process while for the PBSA the photo-ones. By tailoring the percentage of the two comonomeric units in the copolymer it is possible to tune the permeability behavior besides optimizing the chemical–physical properties, in view of the desired application field.

3.4. FT-IR spectroscopic data

FT-IR spectra were also recorded for each sample in order to investigate possible changes in the chemical structure due to the processing. The principal absorption bands in the infrared range are summarised in Table 7 for both films. From the spectra, it can be evicted that no substantial changes are induced by the stressed treatments. It was observed only a small change of the band intensity due to the increasing mobility of the polymer chains and a small shift not more than ±10 cm^{-1} from the standard ones [38]. The main difference was recorded for PBSA sample after photo-oxidation where the peak recorded at 2918 cm^{-1}, associated to the CH stretch of the CH_2 group was more intense after photo-oxidation, as observed also from thermal analysis. Further, an increase of intensity of the band at 1712 cm^{-1}, associated to the C=O group, after aging, cold be an indication of a starting degradation process [12].

4. Conclusion

Permeability data after contact with food simulants indicate a different trend for PBS and PBSA sample. PBS shows an increment of the permeability, especially in ethanol ambient. PBSA permeability on the contrary decreases, mainly in acetic acid. The two polymers are characterized by the same behavior when in contact with distilled water and isooctane, an increment/decrement of the GTR value being observed, respectively.

The results obtained indicate that during the food simulant contact a change of crystalline/amorphous ratio occurs, which however affects the permeability behavior in a different way. Moreover, in this paper we pointed out that a linear correlation between crystallinity and permeability does not always exist, because the sorption (thermodynamic parameter) and diffusivity (kinetic parameter) processes are influenced by others factors, like polymer segments and intersegmental packing, environment (polar or not), temperature, and so on.

Table 7
FT-IR data for PBS and PBSA films.

Chemical group	Peak position, cm^{-1}
-OH stretch (free)	3570
CH- stretch (of CH_2 and CH_3 group)	2918 (ν_{as} CH_2), 2857 (ν_s CH_2)
	2946 (ν_{as} CH_3), 2857 (ν_s CH_3)
-C=O normal carbonyl stretch	1712
-CH- deformation symmetric and asymmetric bending	1473 (δ_s CH_2), 1448 (δ_{as} CH_3)
	1388 (δs CH_3)
C–O–H in-plane bend	1425
-CH_2- scissoring	1388
-C=O bending	1246
-C–O- stretching	1180, 1152
-OH bending	1046
-CH_2, wagging and twisting	1246, 1179
-CH_2 rocking	748
O–H out-of-plane	994 (as), 955 (s)
-C–C- stretch	918, 806

From FT-IR data it was evidenced that no severe damage of the materials was observed even if the samples were exposed to stressed degradation environment like thermo- and photo-oxidative ambient and simulants liquid contact. The results obtained confirm the potentiality of these materials for the food's packaging field. Obviously, many other analyses must be performed to ensure the material safety for food contact.

Lastly, the different behavior shown by the two polymers, can be considered a further evidence that copolymerization is a powerful and efficient strategy to tailor material's final properties as chemical–physical, mechanical and gas barrier properties, to fit well a specific application.

Acknowledgement

The authors thank the Showa Denko for kindly supplied the polymer materials used in this work.

References

[1] Alavi S, Thomas S, Sandeep KP, Kalarikkal N, Varghese J, Yaragalla S. Polymer for packaging application, vol. 2. CRC Press, Taylor & Francis Group; 2014. p. 39–52.
[2] Arvanitoyannis IS. Totally and partially biodegradable polymer blends based on natural synthetic macromolecules: preparation, physical properties, and potential as food packaging materials. J Macromol Sci Rev Macromol Chem Phys 1999;C39(2):205–71.
[3] Atkins P, Jones L. Chemical principles – the quest for insight. 5th ed. New York, USA: Freeman WH & Co.; 2012.
[4] Bocchini S, Battegazzore D, Frache A. Poly(butylenesuccinate co-adipate)-thermoplastic starch nanocomposites blends. Carbohydr Polym 2010;82:802–8.
[5] Bucci DZ, Tavares LBB, Sell I. Biodegradation and physical evaluation of PHB packaging. Polym Test 2007;26:908–15.
[6] DeLeris JP. Water activity and permeability. In: Mathalouthi M, editor. Food packaging and preservation. New York: Elsevier Applied Science; 1986. p. 213–33.
[7] Elvira M, Tiemblo P, Gomez-Elvira JM. Changes in the crystalline phase during the thermo-oxidation of a metallocene isotactic polypropylene. A DSC study. Polym Degrad Stab 2004;83:509–18.
[8] Fabbri M, Gigli M, Gamberini R, Lotti N, Gazzano M, Rimini B, et al. Hydrolysable PBS-based poly(ester urethane)s thermoplastic elastomers. Polym Degr Stab 2014;108:223–31.
[9] Gajdoš J, Galić K, Kurtanjek Ž Ciković N. Gas permeability and DSC characteristics of polymers used in food packaging. Polym Test 2001;20:49–57.
[10] Galić K, Ciković N. Permeability characterization of solvent treated polymer materials. Polym Test 2001;20:599–606.
[11] Gas permeability testing manual, Registergericht Munchen HRB 77020, brugger feinmechanik GmbH. 2008.
[12] Gauthier E, Laycock B, Cuoq FJJM, Halley PJ, George KA. Correlation between chain microstructural changes and embrittlement of LLDPE-based films during photo- and thermo-oxidative degradation. Polym Degrad Stab 2013;98(1):2301–12.
[13] George SC, Thomas S. Transport phenomena through polymeric systems. Prog Polym Sci (Oxford) 2001;26(6):985–1017.
[14] Gigli M, Negroni A, Soccio M, Zanaroli G, Lotti N, Fava F, et al. Influence of chemical and architectural modifications on the enzymatic hydrolysis of poly(butylene succinate). Green Chem 2012;14:2885–93.
[15] Gigli M, Negroni A, Zanaroli G, Lotti N, Fava F, Munari A. Environmentally friendly PBS-based copolyesters containing PEG-like subunit: effect of block length on solid-state properties and enzymatic degradation. React Funct Polym 2013;73:764–71.
[16] Huang SJ. Encyclopedia of polymer science engineering: biodegradable polymers, vol. 2. New York: Wiley-International; 1985.
[17] Jakubowicz I. Evaluation of degradability of biodegradable polyethylene (PE). Polym Degrad Stab 2003;80:39–43.
[18] Jamshidian M, Tehrany EA, Cleymand F, Leconte S, Falher T, Desobry S. Effect of synthetic phenolic antioxidants on physical, structural, mechanical and barrier properties of poly lactic acid film. Carbohydr Polym 2012;87:1763–73.
[19] Kanehashi S, Kusakabe A, Sato S, Nagai K. Analysis of permeability; solubility and diffusivity of carbon dioxide, oxygen and nitrogen in crystalline and liquid crystalline polymers. J Membr Sci 2010;365:40–51.
[20] Koutny M, Lemaire J, Delort AM. Biodegradation of polyethylene films with prooxidant additives, a review. Chemosphere 2006;64:1243–52.
[21] Kumazawa H, Bae SY. Sorption and permeation behaviour for a gas in glassy polymer membrane near the glass transition temperature. J Applyed Polym Sci 1996;60(1):115–21.
[22] Lee DS, Yam KL, Piergiovanni L. Food packaging science and technology. Boca Raton, Fla: CRC Press, Taylor & Francis Group; 2008.
[23] Liu RYF, Hu YS, Schiraldi DA, Hiltner A, Baer E. Crystallinity and oxygen transport properties of PET bottle walls. J Applyed Polym Sci 2004;94(2):671–7.
[24] Lu LX, Xu F. Effects of light-barrier property of packaging film on the photo-oxidation and shelf life of cookies based on accelerated tests. Packag Technol Sci 2009;22:107–13.
[25] Mochizuki M, Mukai K, Yamada K, Ichise N, Murase S, Iwaya Y. Structural effects upon enzymatic hydrolysis of Poly(butylene succinate-co-ethylene succinate)s. Macromolecules 1997;30(24):7403–7.
[26] Morillon V, Debeaufort F, Blond G, Voilley A. Temperature influence on moisture transfer through synthetic films. J Membr Sci 2000;168:223–31.
[27] Mrkić S, Galić K, Ivanković M, Hamin S, Ciković N. Gas transport and thermal characterization of mono- and di-polyethylene films used for food packaging. J Appl Polym Sci 2006;99(4):1590–9.
[28] Nagata M, Goto H, Sakai W, Tsutsumi N. Synthesis and enzymatic degradation of poly(tetramethylene succinate) copolymers with terephthalic acid. Polymer 2000;41(11):4373–6.
[29] Nikolic MS, Djonlagic J. Synthesis and characterization of biodegradable poly(butylene succinate-co-butylene adipate)s. Polym Degrad Stab 2001;74:263–70.
[30] NIST-Natl Inst of Standards and Technology. In: Thompson A, Taylor BN, editors. Guide for the use of the international system of units (SI), special publication 811; 2008 [U.S. Department of Commerce].
[31] Pranamuda H, Tokiwa T, Tanaka H. Microbial degradation of an aliphatic polyester with a high melting Point. Poly(Tetramethylene Succinate)Applied Environ Microbiol 1995;61(5):1828–32.
[32] Regulation (EC) No 1935/2004 of the European Parliament and of the Council of 27 October 2004 on materials and articles intended to come into contact with food and repealing Directives 80/590/EEC and 89/109/EEC.
[33] Regulation (EU) No 10/2011 of 14 January 2011 on plastic materials and articles intended to come into contact with food 2011.
[34] Robertson GL. Food packaging: principles and practice. 2nd ed. New York: Marcel Dekker; 2006.
[35] Romani S, Tappi S, balestra F, Rodriguez-Estrada MT, Siracusa V, Rocculi P, et al. Effect of different new packaging materials on biscuit quality during accelerated storage. J Sci Food Agric 2015;95:1736–46. http://dx.doi.org/10.1002/jsfa.6888. wileyonlinelibrary.com.
[36] Scheichl R, Klopffer M-H, Benjelloun-Dabaghi Z, Flaconnèche B. Permeation of gases in polymers: parameter identification and nonlinear regression analysis. J Membr Sci 2005;254:275–93.
[37] Scott G. Green polymer. Polym Degrad Stab 2000;68:1–7.
[38] Silverstain RM, Blasser GC, Morril TC. Spectrometric identification of organic compounds. 4th ed. New York (United States of America): John Wiley & Sons; 1981.
[39] Siracusa V, Rocculi P, Romani S, Dalla Rosa M. Biodegradable polymers for food packaging: a review. Trends Food Sci Technol 2008;19:634–43.
[40] Siracusa V, Blanco I, Romani S, Tylewicz U, Dalla Rosa M. Gas permeability and thermal behavior of polypropylene films used for packaging minimally processed fresh-cut potatoes: a case study. J Food Sci 2012;77(10):E264–72.
[41] Siracusa V, Blanco I, Romani S, Tylewicz U, Rocculi P, Dalla Rosa M. Poly(lactic acid)-modified films for food packaging application: physical, mechanical and barrier behavior. J Appl Polym Sci 2012;125:E390–401.
[42] Siracusa V. Food packaging permeability behaviour: a report. Int J Polym Sci 2012:1–11.
[43] Song DK, Sung YK. Synthesis and characterization of biodegradable poly(1,4-butanediol succinate). J Appl Polym Sci 1995;56(11):1381–95.
[44] Soccio M, Lotti N, Finelli L, Munari A. Effect of transesterification reactions on the crystallization behaviour and morphology of poly(butylene/diethylene succinate) block copolymers. Eur Polym J 2009;45:171–81.
[45] Soccio M, Lotti N, Gigli M, Finelli L, Gazzano M, Munari A. Reactive blending of poly(butylene succinate) and poly(triethylene succinate): characterization of the copolymers obtained. Polym Int 2012;61:1163–9.
[46] Soccio Michelina, Lotti Nadia, Munari Andrea. Influence of block length on crystallization kinetics and melting behaviour of poly(butylene/thiodiethylene succinate) block copolymers. J Therm Anal Calorim 2013;114(2):677–88.